Mechanics & Industry **18**, 307 (2017)

DOI: 10.1051/meca/2016048
www.mechanics-industry.org

Mechanics & Industry

Experimental and theoretical analysis of (water) permeability variation of nonwoven textiles subjected to compression

Petrica Turtoi[1], Traian Cicone[2] and Aurelian Fatu[3,a]

[1] Military Equipment and Technologies Research Agency, St. Aeroportului, 16, Clinceni, Ilfov, 077025, Romania
[2] University Politehnica of Bucharest, Splaiul Independentei, 313, Bucharest, 060042 Romania
[3] Institut Pprime, University of Poitiers, IUT d'Angouleme, 4 Avenue de Varsovie, 16000 Angouleme, France

Received 19 August 2016, Accepted 9 September 2016

Abstract – This paper presents the experimental determination of permeability for unidirectional in-plane flow through a thin layer of nonwoven porous textile subjected to various rates of compression. The experiments were made on an original device that allows the variation of porous layer compression and pressure differential. The permeability was calculated assuming the validity of Darcy law and, in parallel, Darcy-Forchheimer model. The preliminary results obtained with water show that pressure gradient does not influence sensibly the resistance to flow of the material and Darcy's law is applicable. For permeability-porosity correlation the experimental results were fitted using the well-known Kozeny-Carman equation. Also good correlation was found with other two models derived from Kozeny-Carman.

Key words: Porous material / permeability / Darcy / Darcy-forchheimer / Kozeny-Carman

1 Introduction

It is proven, both theoretically and experimentally, that when a soft porous layer imbibed with a fluid is subjected to compression by a rigid and impermeable component in sliding or normal (approaching) relative motion, high lift forces can be generated. This mechanism is based on the variation of permeability with the porosity: when the porous layer is compressed, the local porosity decreases, and correspondingly, the permeability decreases also, increasing the resistance to flow of the squeezed fluid. The mechanism was named by Pascovici [1] ex-poro-hydrodynamic (XPHD) lubrication and it is characteristic to very soft porous materials where the lift forces generated by the compression of the solid matrix can be neglected.

This process has a wide applicability from squeeze dampers and shock absorbers to protective equipment for impact or pumping devices. The theoretical analysis of this mechanism is based on the correlation of the level of compression of the porous layer with its porosity and corresponding permeability.

For thin layers of porous materials one can analyse the *transverse permeability*, characterising the flow across the porous layer thickness, as well as *in-plane permeability*.

Nomenclature

B, b	Width
C_f	Drag constant (Forchheimer coefficient)
d_f	Fiber diameter
h	Tthickness
h_0	Initial thickness of the porous material
k_{KC}	Kozeny-Carman constant
k_E	Emersleben constant
k_{RG}	Rushton-Green constant
p	Pressure
Re_ϕ	Reynolds number in porous media
v	Velocity
v_m	Mean velocity
x, y, z	Cartesian coordinates
A	Sectional area
L, l	Length
Q	Volumetric flow rate
ε	Porosity
ε_0	Material porosity at initial thickness
η	Dynamic viscosity
ϕ	Permeability
ρ	Fluid density

[a] Corresponding author:
aurelian.fatu@univ-poitiers.fr

For the applications based on the XPHD mechanism, a rigid and impermeable support is used for the thin porous layer. As a consequence, the in-plane flow is preponderant. Because the fluid is expelled out at high pressure gradients, which may vary in time, it is also of interest to evaluate their influence on permeability.

The permeability of a porous structure depends not only on its porosity but also on its morphology (tortuosity, communicating/non-communicating pores [2]), on fluid properties and on fluid-solid matrix interaction. Therefore, despite the existence of many models for porosity-permeability correlation, there is a continuous need for new experiments correlated with the envisaged applications.

The first attempts to elucidate the phenomenon of fluid flow through porous materials were made in geology, stimulated by the applications in oil extraction. Theoretical models have been proposed for both water and oil underground flow through beds of rocks. The porous material models were simplified up to a group of parallel capillaries [3] or a packing of spheres [4]. The theoretical models try to correlate the average pore diameter with permeability. Currently, a lot of theoretical models that correlate the structure of the porous medium with permeability for low porosity materials like textiles and foams can be found in the literature. Applications in the textile industry have a significant contribution, but the studies were focused on the development of methods to determine the transverse permeability of textiles for gases or water. A remarkable evolution in the study of permeability for fibrous, woven or nonwoven textiles occurred in the late twentieth century, with the development of parts manufacture by injection (Resin transfer molding - RTM). Gebart [5] and Parnas and Salem [6] are among the first who made measurements using specialized devices (permeameter) for unidirectional and radial plane flow. For anisotropic woven materials made of fibers, Gebart proposes two directions for determining permeability: perpendicular and parallel. The experimental mould used by Gebart allows resin injection and is made from two parts, an aluminium base and an upper transparent plate assembled with a rubber sealing. Currently there is no standard method for measuring the permeability of the materials in fibers plan [7] although the literature abounds with studies on this topic. It is also unanimously accepted that errors in permeability assessment could be as high as one order of magnitude. A worldwide benchmark organised for the measurement of carbon fabric in-plane permeability using 16 different experimental procedures has shown results in large scatter data, although for each procedure the results appeared consistent [8,9].

It must also be mentioned the experimental studies made by Lundstrom [10] on unidirectional permeability. The device used allows permeability determination for oil flow and high input pressure. The fabric used is a non-crimp stitched fabrics with aligned fibers on two directions. Multiple layers where cut and stacked with fibers aligned to obtain three volume fractions. The results showed that the measured permeability can increase up to three times when the direction of flow is changed.

The present paper presents some experimental results for the water permeability of nonwoven textiles and its variation with porosity and pressure differential. The results are fitted with well known Kozeny-Carman equation and two other related models.

2 Experimental set-up

The device (Figs. 1 and 2) consists of a metallic base, where a rectangular ($L \times B = 300 \times 100$ mm^2) open cavity accurately machined serves as support for the porous layer specimen. The inlet hose and a pressure transducer are connected to the closed side of the cavity. The cavity is covered with a stepped upper plate, used to compress the porous material through its compaction shoulder. The upper plate is transparent to allow visualization of the fluid flow. The surfaces of the two plates in contact with the porous material are parallel within 0.02 mm in order to ensure uniform compression. The device is sealed using an O-ring and a uniform sealing force is applied by using a U-profile steel frame. A valve with gauge is used to set up the input pressure which is accurately measured in the cavity, with the pressure transducer. An adjustable collector divides the flow on the output edge into bulk flow (of effective width $b = 83$ mm) and side flow, respectively. Only the bulk flow is collected for the assessment of the permeability.

The device has similar features if compared with the device built by Lündstrom [10] in terms of fluid collector, pressure inlet and transducer positioning. The particularity of this device is its possibility to measure the rate of flow for different levels of compression of the same specimen. A set of different upper plates with various shoulder depths are used. The maximum compression is limited by the forces generated in order to deform the solid component of the porous material. Beyond that, the device is no more watertight.

The experimental analysis presented in this paper is dedicated to water permeability of felt. This material has a highly compressible structure made of tangled long polyester fibers with relatively uniform diameter. The felt is hydrophobic and the saturated porous structure modifies its initial (dry) dimensions with less than 2%. Using magnified microscopic images, the fibers diameter was found within the range $28 \div 42$ μm and consequently, an average fiber diameter $d_f = 36$ μm was used for the analytical models. Fibers arrangement is random throughout its volume and the material can be assumed homogeneous and isotropic. Based on this, despite that the measurements were made for uni-directional flow, the results are supposed valid regardless of the flow direction. Porous material sheet specimens of initial thickness $h_0 = 7$ mm were cut at $l \times B = 245 \times 100$ mm^2 and fit into the device cavity, aligned to the outer edge. Care was given to the side contact between the specimen and the cavity. Each specimen was anchored to the cavity in order to avoid fluid entrainment at low compression rates and

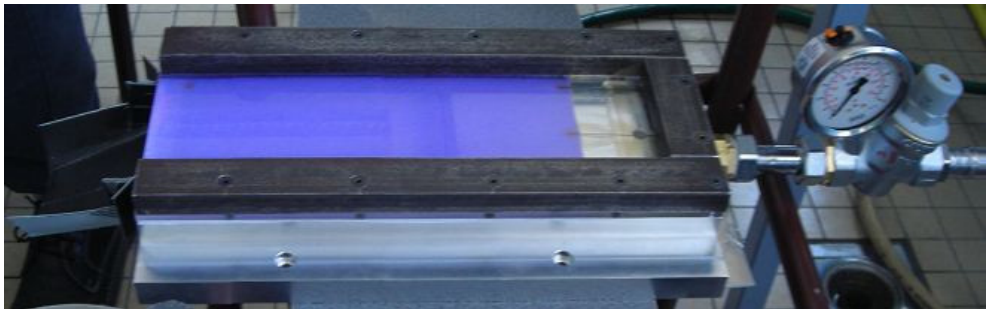

Fig. 1. Experimental device connected to water source.

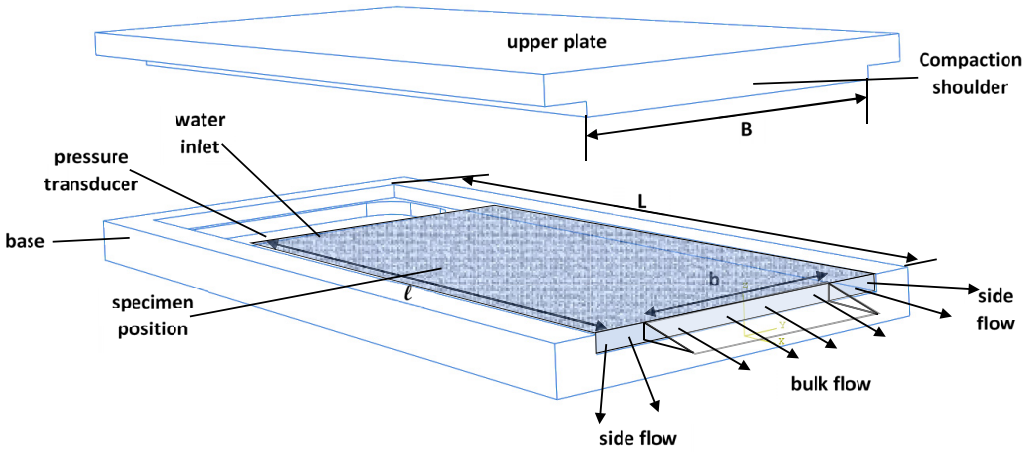

Fig. 2. Schematic of the experimental device.

high pressure differential. The initial porosity $\varepsilon_0 = 0.8$ was measured using a gravimetric method.

Each specimen was dipped in water one day prior to measurements, then placed into the permeameter cavity and compressed successively with different upper plates. Multiple rates of compression were thus obtained, reducing the initial thickness with a maximum factor of 2. The experiments consisted in measuring the volumetric rate of flow by weighing the collected water during a few minutes, function of the rate of compression. The water was collected after the porous material was fully imbibed and the flow stabilized. Each measurement was repeated three times and the averages of the measured values were recorded. The input pressure was varied between 1 and 3 bars. All the measurements were performed at room temperature which was close to 20 °C.

Visualisation through the transparent upper plate has revealed that the flow profile is straight and parallel with the edge in the bulk zone. This profile declines slightly near to the walls, especially at higher pressure differentials.

3 Experimental results

For a set of experimental data, each specimen of porous material was compressed with a different compaction shoulder (Fig. 2) and then the rate of flow was measured for several distinct values of input pressure, up to 3 bars.

In order to correlate the rate of compression with the porosity it is assumed that the in-plane section area ($l \times B$) is constant and independent of the level of compression. Accordingly, if we accept that the solid matrix of the porous layer does not change its volume during compression, the product between porosity and the porous layer thickness is constant:

$$(1-\varepsilon)h = (1-\varepsilon_0)h_0 \tag{1}$$

The experimental volumetric rate of flow function of pressure difference for different porosities calculated with Equation (1) is presented in Figure 3.

In order to determine the permeability from the experimental data, a flow model for the porous medium must be fitted on the measured flow parameters (pressure differential and rate of flow). There are many flow models to be used but, the oldest and the most notorious is the model of Darcy; it is almost unanimously used to fit experimental data. According to Darcy law, the pressure drop over unit length of porous medium is proportional to the dynamic viscosity and fluid mean velocity and inversely proportional to permeability

$$\frac{\mathrm{d}p}{\mathrm{d}x} = \frac{\Delta p}{\ell} = -\frac{\eta}{\phi} v_m \tag{2}$$

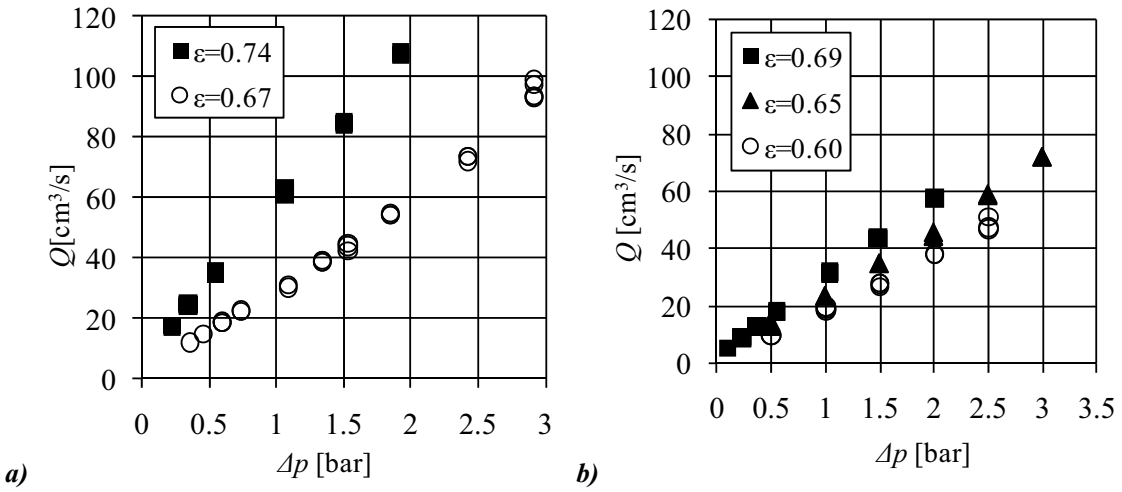

Fig. 3. Flow rate variation versus inlet pressure for different porosities.

Here the mean velocity of the fluid (also called Darcian velocity) is obtained by dividing the rate of flow to the cross-section area of the sample ($A = b \times h$):

$$v_m = Q/A \tag{3}$$

The validity of Darcy law is restricted to laminar, low velocity, flows. This limit is given by the permeability-related Reynolds number:

$$Re_\phi = \frac{\rho\sqrt{\phi}}{\eta} v_m \tag{4}$$

where ρ is the density of the fluid. For $Re_\phi < 1$ the flow is assumed laminar, but values up to 10 can be considered acceptable for the usage of Darcy model.

In consequence, a first attempt to estimate the permeability was made using the Darcy model; this is sustained by the aspect of the curves in Figure 3 where can be seen that the flow rate varies almost linearly with pressure difference. A least-squares linear curve fit through the pressure-drop versus fluid-velocity data points is used to give the Darcy permeability. The viscosity η and the density ρ of the fluid are considered constant and equal to 0.001 Pa.s and 10^3 kg.m^{-3} respectively. Based on this typical procedure the values of permeability were found in a narrow range, between 10^{-10} and 5×10^{-10}. A limitation of the Darcy model is the assumption of constant velocity of the fluid in the porous layer. This can be a reasonable hypothesis for this simple in-plane flow, especially when the side-flow is ignored from the analysis. However, on the boundaries between the porous layer and the upper and lower walls, the fluid velocity goes to zero if a no-slip boundary conditions is considered. This induces a variation of the fluid-velocity with the layer thickness that cannot be predicted with the Darcy model. Therefore, the permeability was also estimated using the Darcy-Brinkman model:

$$\frac{\mathrm{d}p}{\mathrm{d}x} = -\frac{\eta}{\phi} v + \eta_{\text{eff}} \frac{\partial^2 v}{\partial z^2} \tag{5}$$

where η_{eff} is the so-called effective viscosity that is usually calculated as the ratio between the dynamic viscosity and the porosity : $\eta_{\text{eff}} = \eta/\varepsilon$. By integrating Equation (6) the expression of the fluid velocity is written as a function of the porous layer thickness:

$$v\,(z) = G_1 \sinh(\omega z) + G_2 \cosh(\omega z) - \frac{\phi}{\eta}\frac{\mathrm{d}p}{\mathrm{d}x} \tag{6}$$

where G_1 and G_2 are two integration constants and $\omega = \sqrt{\frac{\varepsilon}{\phi}}$. Assuming no-slip boundary conditions, $v\,(z=0) = v\,(z=h) = 0$, Equation (6) becomes:

$$v\,(z) = \frac{\phi}{\eta}\frac{\mathrm{d}p}{\mathrm{d}x}\left[\frac{1-\cosh(\omega h)}{\sinh(\omega h)}\sinh(\omega z) + \cosh(\omega z) - 1\right] \tag{7}$$

The volumetric rate of flow is found by the integration of Equation (7):

$$Q(\phi) = b\int_0^h v\,(z)\,dz = -b\frac{\phi}{\eta}\frac{\mathrm{d}p}{\mathrm{d}x}\left[h - 2\frac{1-\cosh(\omega h)}{\omega\sinh(\omega h)}\right] \tag{8}$$

A least-squares curve fit through the rate of flow versus the pressure difference is used to give the Darcy-Brinkman permeability. It is important to note that, similar to the Darcy model, the variation of the volumetric rate of flow is still considered linear with the pressure gradient.

Figure 4a shows the results obtained in terms of permeability for Darcy and Darcy-Brinkman models. It can be observed that the differences are very small (less than 1.2%) which leads to the conclusion that Darcy-Brickman model does not bring any important corrections in estimating the permeability. This can be explained by Figure 4b that shows the fluid-velocity variation versus the porous medium thickness at $\varepsilon = 0.6$. The differences are only limited to a very thin layer near the boundaries between the porous layer and walls where the Darcy-Brickman model respects the no-slip condition.

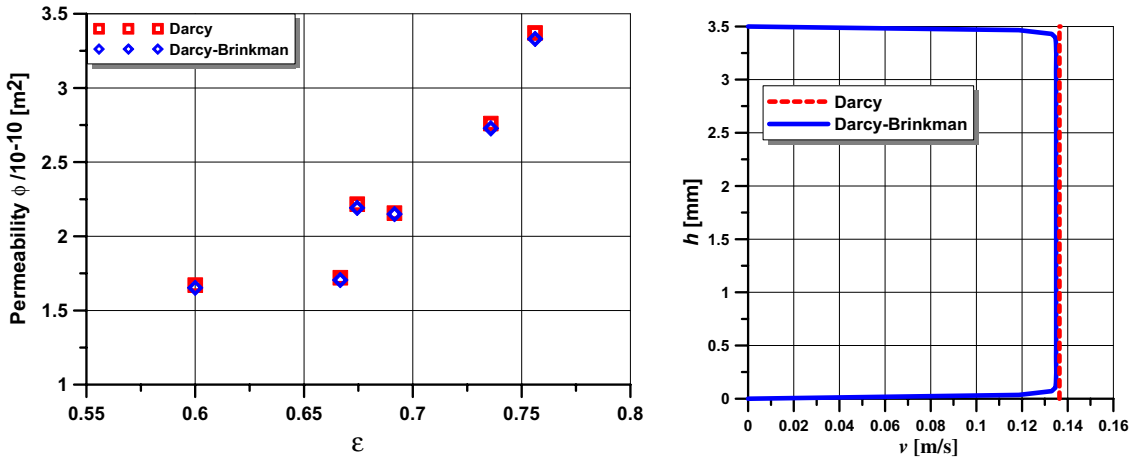

Fig. 4. (a)Permeability variation versus porosity for Darcy and Darcy-Brickman models; (b)Velocity profile for Darcy and Darcy-Brickman models at $\varepsilon = 0.6$.

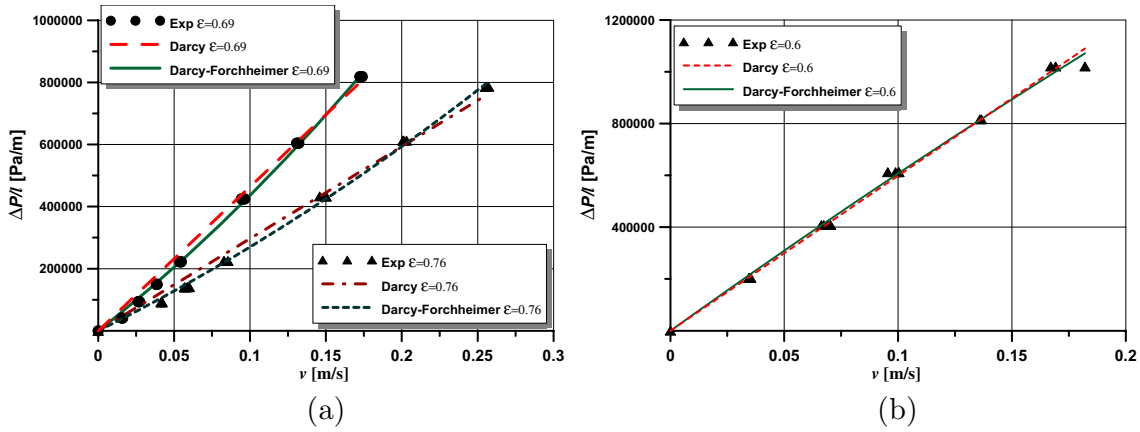

Fig. 5. Experimental pressure-drop versus fluid-velocity fitted with Darcy and Darcy-Forchheimer models.

An in-depth analysis of the experimental results depicted in Figure 3 shows that at higher porosity, the variation of the flow rate slightly deviates from a straight line. Therefore, it was considered necessary to analyse the influence of inertia effects, including into the Darcy law the Dupuit-Forchheimer term, which counts for drag forces [11]. Accordingly, the pressure drop over unit length becomes:

$$\frac{\mathrm{d}p}{\mathrm{d}x} = \frac{\Delta p}{l} = -\frac{\eta}{\phi} v_m - \frac{C_f \rho}{\sqrt{\phi}} v_m^2 \tag{9}$$

where C_f represents a constant (named also drag constant) that varies with the porosity of the medium. In this case, the variation of the pressure gradient with the fluid velocity is parabolic. A least-squares parabolic curve fit through the pressure-drop versus fluid-velocity is used to give both the Darcy-Forchheimer permeability and the drag constant.

Figure 5 shows the results and the corresponding data fits for three different levels of compression of the porous specimen. It can be observed that for relatively low compression ($\varepsilon = 0.69$ and $\varepsilon = 0.76$), the Darcy-Forchheimer model shows a better correlation with the experiments. For higher levels of compression both models give almost equivalent results.

A comparison between the permeabilities predicted with both models is synthetically shown in Figure 6. It can be seen that the differences between determined values increase with the increase of the porosity. When the fluid flows more rapidly, the local inertial effect becomes non-negligible. Consequently, the Darcy-Forchheimer law becomes more precise.

It can be interesting to define the transition of the pressure-drop from a linear to quadratic curve. A factor commonly used to determine the transition is the permeability-related Reynolds number, given by Equation (4). This can be coupled with a different representation of data from Figure 5. Equation (9) can be rewritten as:

$$\frac{\Delta p}{l v_m} = -\frac{\eta}{\phi} - \frac{C_f \rho}{\sqrt{\phi}} v_m \tag{10}$$

The result is graphically represented in Figure 7a for $\varepsilon = 0.76$ and in Figure 7b for $\varepsilon = 0.6$. The discrete data points are experimentally obtained and the lines which

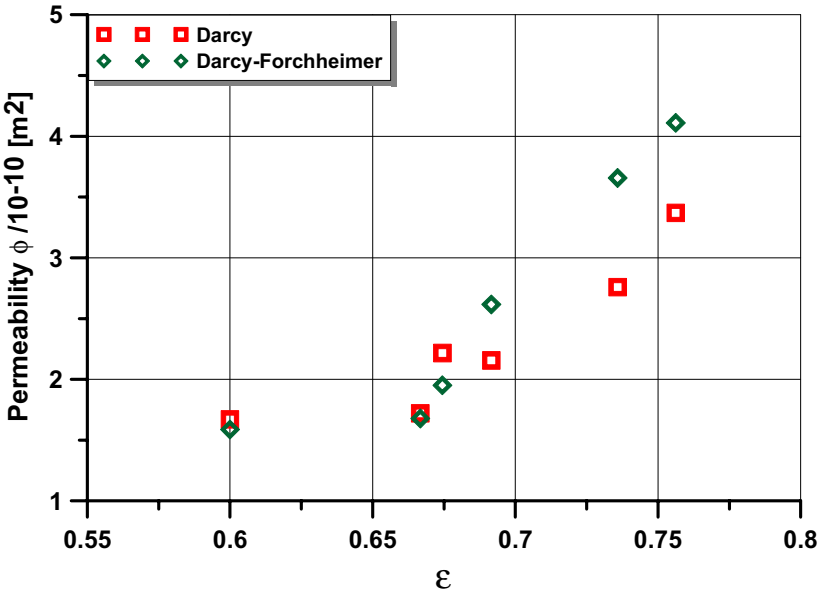

Fig. 6. Comparison between permeability determined using Darcy and Darcy-Forchheimer law.

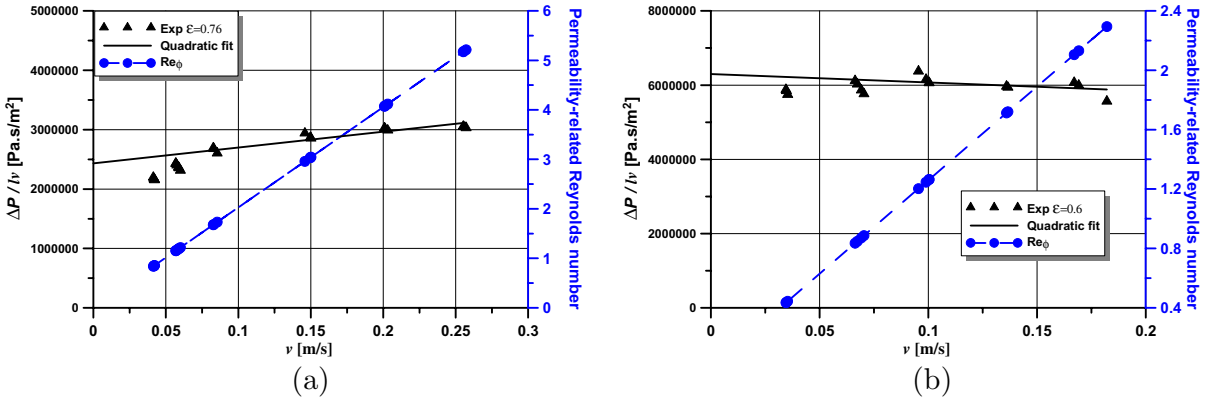

Fig. 7. Experimental variation of $\Delta p/lv_m$ and of Reynolds number versus fluid-velocity.

are shown passing through the points are the second-order curves fitted to the pressure-drop data points using the curve-fitting technique and represented in Figure 5. For each experimentally obtained point, the permeability-related Reynolds number is also represented on a second axis.

If the coefficient of velocity in the right-side member of the Equation (10) is negligible, the data points must describe a horizontal line which means that the flow can be defined by the simple Darcy model. This can be observed in Figure 7b. When the drag coefficient, C_f, becomes important, the data points must describe a positive slope, that seems to be the case in Figure 7a. In this case, the flow regime is no longer Darcian and the Forchheimer correction must be integrated for the experimental data interpretations. However, the positive slope observed in Figure 7a is not really prominent which means that, even for the highest tested fluid velocity, we are still in a transient flow regime. Supplementary tests at higher fluid velocity are necessary to completely exceed the Darcian flow regime. Concerning the modified Reynolds number, it can be noticed that for values greater than 2, a non-Darcian flow regime can be expected.

4 Porosity-permeability correlation models

Further exploitation of the experimental data was dedicated to the accuracy of some analytical correlations between porosity and permeability. The quasi-empirical Kozeny-Carman (KC) equation is the most famous and widely used for this correlation. Originally developed for porous media formed by spherical particles, it was modified by Ghaddar for flow through fibers of constant diameters, d_f [12] and has the following form:

$$\phi_{KC} = \frac{d_f^2 \varepsilon^3}{16\, k_{KC}\, (1-\varepsilon)^2} \tag{11}$$

where for the constant k_{KC} values between 5 to 10 were recommended.

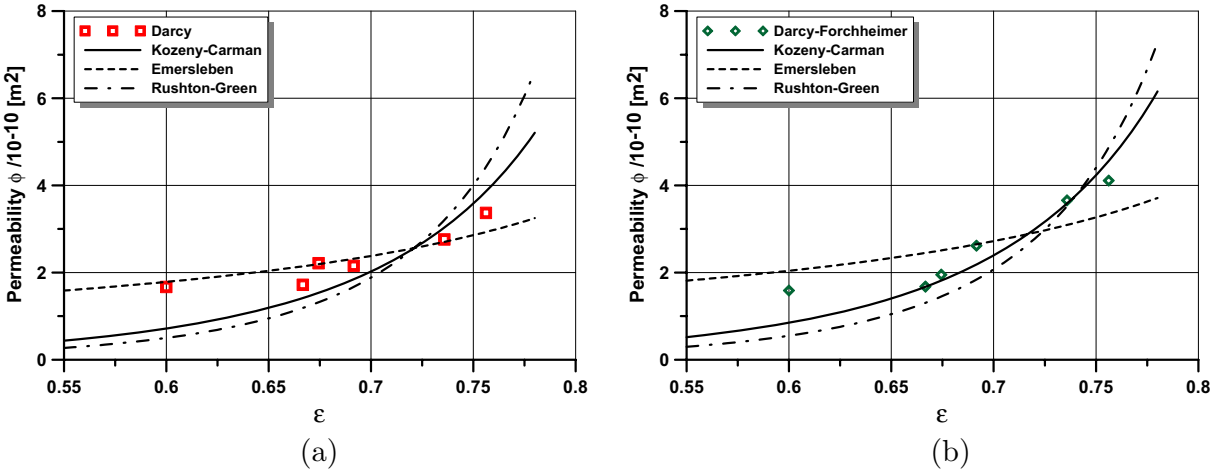

Fig. 8. Permeability variation versus porosity for Kozeny-Carman, Emersleben and Rushton-Green fitted from experimental results obtained with Darcy (a) and Darcy-Forchheimer (b) models.

Table 1. Kozeny-Carman constant and related obtained by least square fit for permeability calculated with Darcy and Darcy-Forchheimer models.

Model	Darcy	Darcy-Forchheimer
Kozeny-Carman	$k_{KC} = 1.53$	$k_{KC} = 1.29$
Emersleben	$k_{EM} = 18.14$	$k_{EM} = 15.87$
Rushton-Green	$k_{RG} = 5.46$	$k_{RG} = 4.97$

Two other models which were derived from Kozeny-Carman equation were also evaluated:

– the Emersleben(EM) model [13]:

$$\phi_{EM} = \frac{d_f^2}{k_{EM}(1-\varepsilon)}, \tag{12}$$

where the value $k_{EM} = 16$ is recommended .

– the Rushton-Green model (RG) [14]:

$$\phi_{RG} = \frac{d_f^2 \varepsilon^3}{16\, k_{RG}\, (1-\varepsilon)^3} \tag{13}$$

Rushton-Green model is applicable for isotropic media and was obtained using a modified Kozeny-Carman constant:

$$k_{RG} = (1-\varepsilon) k_{KC} \tag{14}$$

Based on least square fit method, the coefficients in Kozeny-Carman, Emersleben and Rushton-Green equations were calculated and the values are presented in Table 1. The predicted permeability using the three models, along with the experimental results determined with Darcy, and Darcy-Forchheimer models are graphically represented in Figures 8a and 8b, respectively.

Taking into account the previous results that lead to a better fit of the experimental data using Darcy-Forchheimer law at high porosity, it is evident from Figure 8b that Kozeny-Carman equation is best suited for permeability-porosity correlation. However, attention must be given to the constant in this equation, which may take very different values for various materials. For example, in our case, these values are several times lower than those recommended in the literature.

On the other hand, if a simple Darcy law is used for permeability calculation, Emersleben equation appears to better fit the experimental data.

These different results are reasonable, if we remark that our experiments have been done at transitional regimes of flow, clearly shown by the values of modified Reynolds number.

5 Conclusions

An original experimental study was presented in this paper, dedicated to the assessment of the permeability for soft materials subjected to compression. The experimental device allows the measurement of the unidirectional flow rate at relative high input pressure and for various compression rates. The validity of Darcy law was verified and it was shown that Darcy-Forchheimer law offers a better correlation with experimental data for higher mean velocity (>0.2 m.s^{-1}) which corresponds to higher porosity. The predicted permeabilities obtained with each model (Darcy and Darcy-Forchheimer, respectively) differ with a factor less than 1.5 (differences less than 50%) a result which can be considered acceptable, taking into account that results scatter of up to one order of magnitude are considered acceptable [8, 9]. Also, Kozeny-Carman equation was used to fit permeability results and the constant determined was much smaller than the recommended one. Other two related equations were analysed. Emersleben equation shows the best correlation with the experimental data if Darcy law is used for permeability calculation. However, care must be taken when an equation relating permeability and porosity is extended on a large interval of porosity values. It is also very important to evaluate for each set of experimental data which of the flow models are best suited.

Acknowledgements. This work was supported by MEN-UEFISCDI Partnership Program PN-II Contract No 287/2014 (PROTHEIS).

References

[1] M.D. Pascovici, Lubrication by dislocation: A new mechanism for load carrying capacity, Proceedings of the 2nd World Tribology Congress, Vienna, 41, 2001
[2] A.E. Sheidegger, The physics of flow through porous media, University of Toronto Press, 1974
[3] H. Darcy, Les fontaines publiques de la ville de Dijon, Paris/ Dalmont, 1856
[4] P.C. Carman, Fluid flow through granular beds, Transactions, Institution of Chemical Engineers, London, 15 (1937) 150–166
[5] B. Gebart, Permeability of unidirectional reinforcement for RTM, J. Compos. Mater. 26 (1992) 1100
[6] R.S. Parnas, A.J. Salem, A comparison of the unidirectional and radial in-plane flow of fluid through woven composites reinforcements, Polym. Comp. 14 (1993) 383
[7] P. Ferland, Concurrent methods for permeability measurements in resin transfer molding, Polym. Compos. 17 (1996)
[8] R. Arbter, et al., Experimental determination of the permeability of textiles: A benchmark exercise, Compos. Part A 42 (2011) 1157–1168
[9] N. Vernet, et al., Experimental determination of the permeability of engineering textiles: Benchmark II, Compos. Part A 61 (2014), 172–184
[10] T.S. Lundström, The permeability of non-crimp stitched fabrics, Composi. Part A 31 (2000) 1345-1353
[11] K. Boomsma, D. Poulikakos, The Effects of Compression and Pore Size Variations on the Liquid Flow Characteristics in Metal Foams, J. Fluid Eng. 124 (2002) 263–272
[12] C.K. Ghaddar, On the permeability of unidirectional fibrous media: A parallel computational approach, Phys. Fluids 7 (1995)
[13] V.O. Emersleben, Das Darcysche Filtergesetz, Pshyz Z. 26 (1925) 601–610
[14] A. Rushton, D.J. Green, The analysis of textile filter media, Filtration Separation 5 (1968) 516–523